

FRAP Analysis of the Stability of the Microtubule Population Along the Neurites of Chick Sensory Neurons

Kathryn J. Edson, Soo-Siang Lim, Gary G. Borisy, and Paul C. Letourneau

Department of Cell Biology and Neuroanatomy, University of Minnesota, Minneapolis (K.J.E., P.C.L.); Molecular Biology Laboratory, University of Wisconsin, Madison (S.-S.L., G.G.B.); Friedrich-Miescher Institut, Basel, Switzerland (K.J.E.); and Department of Anatomy, Indiana University Medical Center, Indianapolis, Indiana (S.-S.L.)

In order to study microtubule turnover in elongating neurites, chick embryo sensory neurons were microinjected with x-rhodamine tubulin, and after 6–12 hours, short segments along chosen neurites were photobleached at multiple sites. Previous studies [Lim et al., 1989; 1990] indicated that recovery of fluorescence (FRAP) in neurites occurs by the dynamic turnover of stationary microtubules. In all cases, distal bleached zones recovered fluorescence faster than bleached zones more proximally located along the same neurites. Bleached zones at growth cones completely recovered in 30–40 minutes, while bleached zones located more proximally usually recovered in 50–120 minutes. In the most proximal regions of long neurites, recovery of fluorescence was often incomplete, indicating that a significant fraction of the microtubules in these regions were very stable. These studies indicate that there are differences in microtubule stability along the length of growing neurites. These differences may arise from the combined effects of 1) modifications that stabilize and lengthen microtubules in maturing neurites and 2) the dynamic instability of the distally oriented microtubule plus ends.

© 1993 Wiley-Liss, Inc.

Key words: microtubule dynamics, photobleaching, neurite elongation, microtubule stability

INTRODUCTION

Microtubules are the major cytoskeletal components of developing neurons [Letourneau, 1989]. They have important roles in supporting and maintaining highly extended axonal and dendritic processes. In order to understand how neuronal morphogenesis occurs, it is necessary to understand how microtubular structures are established and maintained. The results reported here address the issues of microtubule organization and turnover in growing nerve fibers.

As a neurite elongates, microtubules must be continuously supplied to the advancing neurite tip. One means for advancing the microtubular cytoskeleton is net microtubule assembly in a growing neurite. Assembly of tubulin occurs within elongating neurites at the plus ends of neuritic microtubules [Okabe and Hirokawa, 1988; Baas and Black, 1990], which are uniformly oriented

toward the neurite terminus [Burton and Paige, 1981; Heidemann et al., 1981; Baas et al., 1987; 1988]. A variety of evidence indicates that the neurite tip contains tubulin subunits and is the prevalent site of microtubule assembly in elongating neurites [Bamburg et al., 1986; Gordon-Weeks, 1987; Gordon-Weeks and Mansfield, 1991]. Thus, net assembly of tubulin into microtubules at the neurite tip may be a major means of forming microtubules in a growing neurite. Another means of microtubule advance is by net translocation of assembled microtubules, a long-standing hypothesis that was pro-

Received September 25, 1992; accepted December 30, 1992.

Address reprint requests to Paul C. Letourneau, Department of Cell Biology and Neuroanatomy, 4-135 Jackson Hall, University of Minnesota, Minneapolis, MN 55455.

posed as underlying axonal transport in mature axons [Hoffman and Lasek, 1975; Lasek, 1986].

Investigations of microtubule translocation in growing neurites have generated conflicting results. Examinations of fluorescence recovery after photobleaching (FRAP) in PC12 cells and in mouse and chick neurons injected with fluorescent analogues of tubulin have indicated that the microtubular network is stationary in elongating neurites [Lim et al., 1989; Lim et al., 1990; Okabe and Hirokawa, 1990], although microtubules may turn over in neurites by the process known as dynamic instability [Mitchison and Kirschner, 1988]. Another approach used photoactivation of fluorescence on labeled tubulin to tag microtubules locally in growing neurites of frog neurons [Reinsch et al., 1991]. Those results suggested a different conclusion, that is, microtubules do move distally in elongating neurites. A subsequent report used photoactivation methods to investigate microtubule movement in both frog and mouse neurons [Okabe and Hirokawa, 1992]. The results from that study support both sides of the conflict. Microtubules move distally in growing frog neurites, but microtubules are stationary in growing mouse neurites. Thus, the conflict can be resolved by proposing that microtubule translocation is not required for neurite elongation, and that both microtubule assembly and translocation can contribute to the formation of the cytoskeleton in neurite elongation.

In fibroblastic cells, microtubules are dynamic polymers, undergoing frequent assembly and disassembly at microtubule ends [Sammak and Borisy, 1988b; Schulze and Kirschner, 1988]. An important aspect of the establishment of stable, elongated neurites may involve mechanisms that stabilize microtubules. Neuritic microtubules may be stabilized by several posttranslational modifications of tubulin, as well as by interactions with several microtubule associated proteins (MAPs) found in neurites [reviews by Matus, 1988; Bulinski and Gunderson, 1991; and Cambray-Deakin, 1991]. Regional analyses of these modifications of microtubules indicate that microtubules in the terminal growth cones are predominantly newly formed, whereas stabilized microtubules are present in more proximal regions of neurites [Robson and Burgoyne, 1989; Arregui et al., 1991]. Similarly, the results of FRAP analyses indicated that microtubules in growth cones of differentiated PC12 cells are labile and turn over within a few minutes [Lim et al., 1989]. These findings support the hypothesis that at neurite tips there is substantial assembly of tubulin into labile microtubules, associated with the motility of growth cones, and that by subsequent modifications the recently formed labile microtubules are transformed into stable neuritic microtubules [Mitchison and Kirschner, 1988].

In a further examination of microtubules in living cultured neurons, we report in this article studies of microtubule dynamics in elongating neurites of chick embryo dorsal root ganglion (DRG) neurons injected with x-rhodamine-tubulin. We examined microtubule movement and turnover rates in different parts of growing neurites. Microtubule turnover rates at different locations were determined by analyzing fluorescence recovery after photobleaching multiple regions of fluorescently labeled microtubules in individual neurites and their growth cones. We found that microtubule turnover at distal locations is always faster than at proximal sites of the same neurite, and that microtubule turnover in growth cones is especially rapid. In addition, an especially stable population of microtubules appears to be located in the proximal portions of longer, more mature neurites.

MATERIALS AND METHODS

Cell Culture

Cultures of sensory neurons were prepared from dorsal root ganglia of E13 chicken embryos, as described previously [Letourneau, 1975; Lim et al., 1990]. To facilitate multiple viewing of the same neuron, the coverslips were overlaid with an electron microscopic locator grid, and carbon was evaporated onto the substratum to produce a pattern. Once plated onto the dishes, the cells were allowed to incubate for 6–12 hours before microinjection.

Microinjection

X-rhodamine labeling of purified brain tubulin was performed as described in Sammak and Borisy [1988a; 1988b]. Just before use, an aliquot of x-rhodamine-tubulin was thawed and spun at 20,000 g for 30 minutes to remove particles and aggregates. To ensure maximal incorporation of tubulin into microtubules of neurites, only cells without neurites or with newly sprouted neurites were chosen for microinjection. The injected volumes were estimated to be less than 10% of the volume of the neuronal perikarya, and the injection process did not cause discernable distortions of the neuronal perimeters. Microinjected cells were then allowed to incubate and extend neurites for 6–12 hours in the incubator before photobleaching. An injected cell was selected and then photobleached one or more times. Phase contrast and fluorescent images were taken before and after photobleaching to record the progress of the neuron during recovery of the bleached zones.

Photobleaching

The photobleaching apparatus, which used an argon ion laser and a Zeiss IM35 microscope (Carl Zeiss, Inc., New York), was assembled as described in Lim et

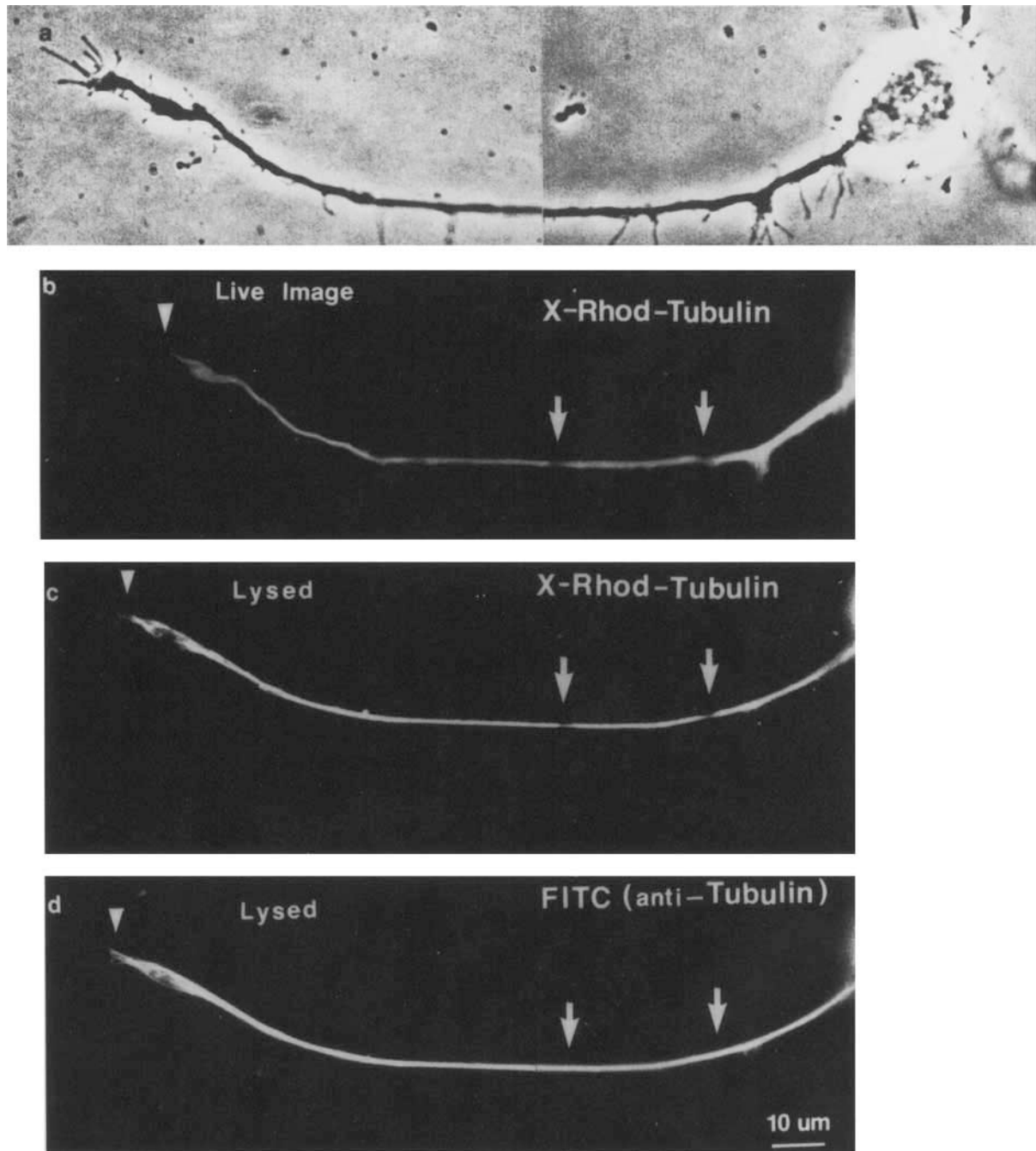


Fig. 1. Photobleaching of x-rhodamine-tubulin does not disrupt x-rhodamine labeled microtubules. See also Fig. 2 for high magnification images of this neuron. A cultured E13 DRG neuron was injected with x-rhodamine-tubulin and returned to the incubator for 6 hours to allow for neurite extension. Three areas along the neurite ($3 \mu\text{m}$ wide) were photobleached using an argon laser set at the minimum intensity that produced a measurable bleached zone. Live images of the neuron (a,b) were recorded, and 20–30 minutes after photobleaching the cell was lysed, fixed (c), and processed for indirect immunofluorescence using a mouse anti- β -tubulin antibody and an FITC-conjugated anti-mouse secondary antibody to stain total tubulin (d). (a) Phase contrast image of live DRG neuron 10 minutes after photobleaching. (b) Corresponding direct rhodamine fluorescence image

of the same neuron 10 minutes after photobleaching at two locations along the neurite (arrows) and once at the growth cone (arrowhead), using laser intensities in the range used for all experiments (100–200 MW for 100–200 msec). (c) Direct rhodamine fluorescence image of the same neuron lysed and fixed 20–30 minutes after photobleaching. When soluble x-rhodamine-tubulin is extracted, the bleached zones are more easily distinguished. The remaining rhodamine fluorescence is x-rhodamine-tubulin incorporated into intact microtubules. (d) The corresponding fluorescein fluorescence image of anti-tubulin staining of the same neurite shows all microtubules. Fluorescein staining is continuous through the bleached zone, indicating that microtubules are not disrupted.

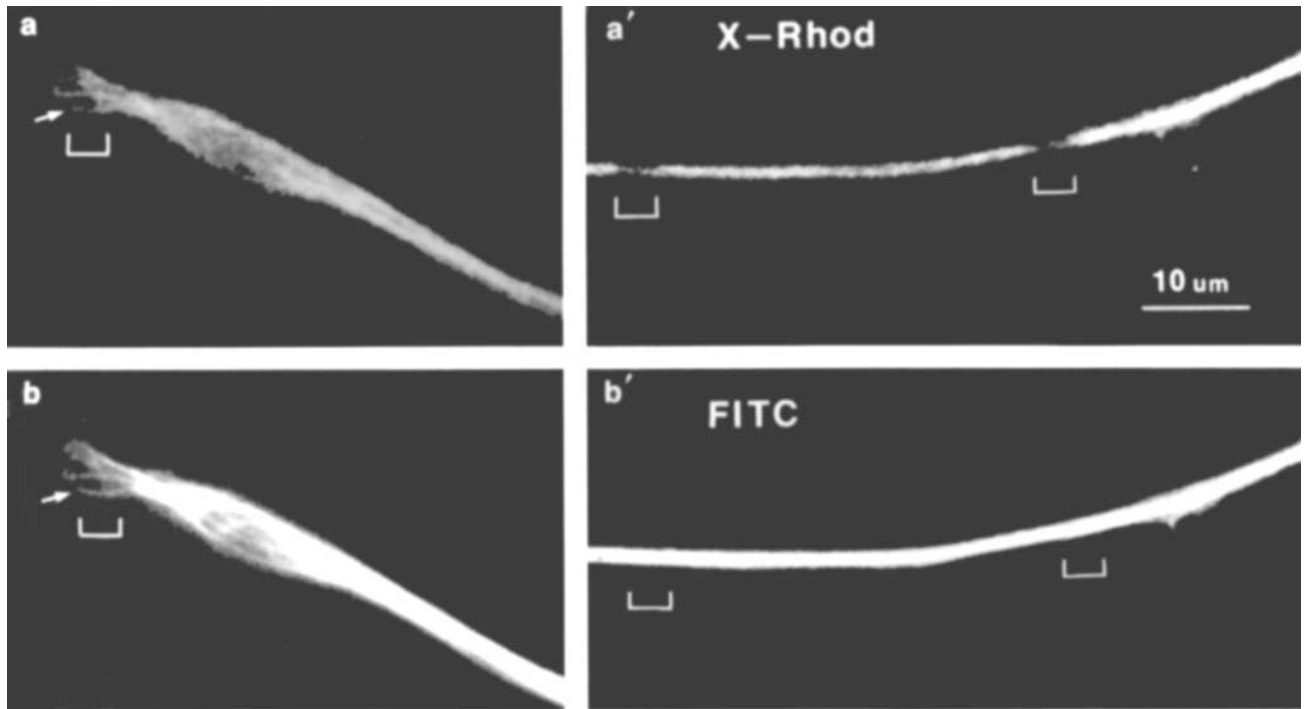


Fig. 2. Microtubules are continuous throughout the bleached areas. (a,a') Direct rhodamine fluorescence of a lysed and fixed DRG neuron. (b,b') Corresponding anti-tubulin fluorescein indirect immunofluorescence images. The lysed, fixed cell described in Fig. 1 is shown in higher magnification images of the x-rhodamine labeled (a,a') and anti-tubulin stained (b,b') microtubules to provide a clearer view of the bleached areas (brackets). Microtubules in neurite shaft

(a',b') are dense and bundled, making it impossible to see individual fluorescent microtubules. However, growth cones (a,b) are flatter and contain splayed microtubules, making it possible to identify individual microtubules or small microtubule bundles (a,b, [arrows]). Comparison of the left panels (a,b) shows that the injected x-rhodamine-tubulin (a) has been incorporated into intact microtubules (arrow), labeled by anti-tubulin-fluorescein antibodies (b).

al. [1989], according to the method of Petersen et al. [1986]. A cylindrical lens was focused to produce a $3 \times 57 \mu\text{m}$ beam in the specimen plane, when using a neofluor $100\times$, 1.3 NA objective. The laser intensity at the specimen, as measured with an optometer (Model 370; United Detector Technology, Hawthorne, CA), was 150–200 MW for 100–200 milliseconds. This irradiation resulted in about a 50–70% reduction in fluorescence relative to the flanking neurite. This exposure ($150 \text{ MW/mm}^2 \times 150 \text{ milliseconds} = 22.5 \text{ MJ/mm}^2$) was about sixfold less than the exposure reported to cause dissolution of purified microtubules in vitro ($71 \text{ MW/mm}^2 \times 2 \text{ seconds} = 142 \text{ MJ/mm}^2$) [Vigers et al., 1988]. This degree of photobleaching was adequate for determining recovery rates and lessens the potential of photodamage by laser light energy.

Image Acquisition and Display

To prevent excessive irradiation, cells were observed by fluorescence only at intervals that varied from 10–90 minutes. The microscope was equipped with a $25\times$ objective and illuminated with a 100 W mercury arc lamp, and the light was passed through ultraviolet

and infrared blocking filters, neutral density filters, and a wide band Zeiss rhodamine filter set. Images of cells were focused with the aid of an SIT camera (Dage-MTI, Michigan City, IN) and an image processor (Quantex, Sunnyvale, CA). A CCD camera, attached to the side port of the microscope with a $5\times$ ocular and a Tokina 80–200 mm zoom lens, was used to record both fluorescent and phase contrast images. This series 200 CCD camera (Photometrics, Ltd., Tucson, AZ) contained a 384×576 pixel chip that was thermoelectrically cooled to -50°C to reduce the dark current noise, and images were digitized to 14-bit depth. After initial storage on the hard drive of a personal computer, digital image files from the CCD camera were stored on a WORM drive optical disc (Model 3363; IBM Corp., Danbury, CT). Photographs for publication were produced from a high resolution monochrome monitor (Sierra Scientific, Mountain View, CA) on Technical Pan 2415 film.

Data Analysis

Measurements of fluorescence intensity along neurites were made from images that were corrected for background noise, camera-related variation in illumina-

TABLE I. Summary of Neurite FRAP Analysis

| Cell | Bleach no. | Bleach site (μm from tip) | L(μm) | R _{max} | t ^{1/2} |
|------|------------|---------------------------------------|--------------------|------------------|------------------|
| A | | 0 | 65 | 100 | 12 |
| B | | 2 | 42 | 100 | 6 |
| C | 1 | 2 | 135 | 100 | 23 |
| | 2 | 45 | — | 100 | 30 |
| | 3 | 73 | — | 100 | 30 |
| | 4 | 104 | — | 100 | 50 |
| D | 1 | 8 | 125 | 100 | 6 |
| | 2 | 108 | — | 80 ^a | 30 |
| E | | 20 | 31 | 100 | 20 |
| F | | 35 | 96 | 95 | 35 |
| G | | 35 | 80 | 100 | 30 |
| H | | 36 | 58 | 95 | 40 |
| I | | 40 | 80 | 100 | 45 |
| J | | 40 | 71 | 100 | 15 |
| K | 1 | 45 | 448 | 100 | 35 |
| | 2 | 336 | — | 70 ^a | 200 |
| L | | 48 | 55 | 100 | 40 |
| M | 1 | 48 | 115 | 100 | 25 |
| | 2 | 103 | — | 100 | 43 |
| | 3 | 112 | — | 100 | 43 |
| N | | 52 | 70 | 100 | 25 |
| O | 1 | 70 | 260 | 100 | 60 |
| | 2 | 145 | — | 70 ^a | 90 |
| | 3 | 229 | — | 70 ^a | 120 |
| P | 1 | 77 | 180 | 100 | 50 |
| P | 2 | 128 | — | 100 | 110 |
| Q | 1 | 82 | 100 | 95 | 117 |
| | 2 | 88 | — | 70 ^a | 117 |
| R | | 105 | 130 | 100 | 50 |
| S | 1 | 105 | 319 | 100 | 20 |
| | 2 | 214 | — | 50 ^a | 140 |
| T | | 106 | 170 | 50 ^a | 120 |
| U | | 127 | 150 | 75 ^a | 90 |
| V | | 139 | 170 | 50 ^a | 100 |
| W | | 146 | 205 | 95 | 150 |
| X | | 209 | 240 | 65 ^a | 130 |
| Y | | 218 | 234 | 100 | 60 |
| Z | | 240 | 250 | 80 ^a | 60 |
| AA | | 252 | 290 | 80 ^a | 60 |
| BB | 1 | 320 | 426 | 95 | 45 |
| | 2 | 358 | — | 95 | 45 |

^aCases where recovery was 80% or less.

This table reports the position of bleached site, total neurite length, extent of fluorescence recovery, and half-time to recovery for all cases where reliable data were obtained. Bleach site = Position of bleached site behind the neurite tip (μm). L(μm) = Length of neurite at beginning of experiment. R_{max} = Maximum percent recovery of fluorescence. t^{1/2} = Time at which bleach zone has recovered to 50% of fluorescence of flanking neurite.

tion (flat-fielding), and bleaching during image acquisition. Fluorescence recovery after photobleaching was assayed by determining the ratio of the radiance in the bleached zone to that in adjacent unbleached regions of the neurite. Background levels were determined by measuring the fluorescence intensity in a region of the substratum adjacent to the fluorescent neurite. Measurement

of the position of a bleached zone was made relative to the neuronal perikaryon, branch points, and other landmark features of the images. Measurements of neurite elongation were taken during times when the bleached zones were still visible.

Indirect Immunofluorescence

Dorsal root ganglion cells were processed for indirect immunofluorescence, as previously described [Lim et al., 1989]. The anti- β tubulin antibody was purchased from Accurate Chemical and Scientific Corp., Westbury, NY.

RESULTS

Experimental Design and Rationale

In order to label uniformly all neuritic microtubules of a neuron with incorporated x-rhodamine-tubulin, we injected cultured chick DRG neurons (E13-14) with x-rhodamine-tubulin after they had attached to the substratum, but before they had extended processes. To determine whether there were local differences in microtubule turnover rates or stability along individual neurites, we photobleached multiple sites along a neurite. Microtubule turnover times were compared by analyzing the rate of fluorescence recovery after photobleaching at these different sites.

Photobleaching was done with an argon laser attenuated to produce a measurable bleached area, to between 20–40% of the initial fluorescence intensity level. Neurites that were photobleached even at multiple sites continued to elongate at rates comparable to those of control cells that were not bleached, indicating that the cells were not detectably damaged by the experimental manipulations. The laser light levels that were used were well below those which have been shown to cause the breakage of microtubules [Vigers et al., 1988]. When cells were photobleached under these conditions and then fixed and detergent-extracted to remove soluble tubulin, indirect immunofluorescence staining with anti-tubulin and fluorescein-conjugated secondary antibodies showed that microtubules were continuous throughout the bleached region (Figs. 1, 2a', 2b'). Other studies, using light and electron microscopy, also demonstrated that microtubules in fibroblasts remained intact through regions that were photobleached under the same conditions [Gorbsky and Borisy, 1989; Centonze and Borisy, 1989].

These observations of continued neuronal growth and microtubule continuity through bleached zones indicate that our method of photobleaching has not damaged neuritic microtubules. However, we do acknowledge that we may not have detected subtle damage to microtubules, which may affect their turnover. A low amount

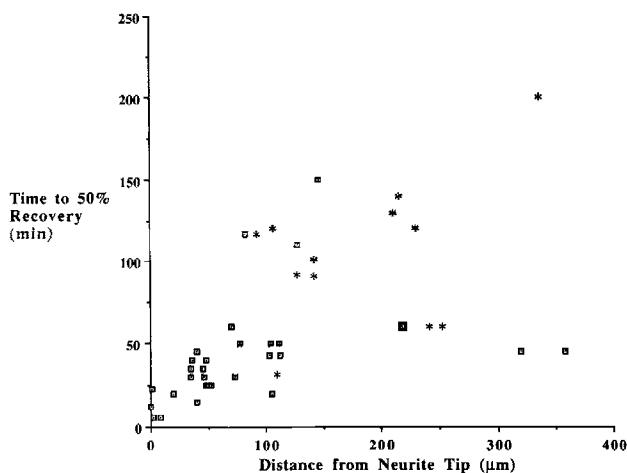


Fig. 3. In this figure the data reported in the table are graphed to illustrate the relationship of fluorescence recovery to the distance that a bleached site was behind the neurite tip. The time for 50% recovery of fluorescence in a bleached area is plotted vs. the position of the bleached area behind the neurite tip. Forty-one bleached sites on 28 neurites are plotted. This graph illustrates the general trend that recovery of fluorescence is more rapid closer to the neurite tip. The graph also shows a feature of the extent of fluorescence recovery. Nineteen of 20 bleached sites within 100 μm of the neurite tip recovered 100% of their initial level of fluorescence. This indicated that the microtubule population in the distal regions of neurites is dynamic. However, 11 of 21 bleaches located more than 100 μm proximal to the neurite tip recovered no more than 80% of their initial fluorescence (asterisks). These results suggest that the proximal regions of neurites contain a subset of very stable microtubules.

of absorbed laser energy may not acutely disrupt the microtubule lattice, but a conformational change induced in tubulin subunits may alter the kinetics of dissociation of irradiated x-rhodamine-tubulin from microtubule ends. It is unknown whether this occurs, or how this affects our basic observation that recovery from photobleaching characteristically varies as a function of position along a neurite.

Axonal Microtubules Are Stationary and Dynamic

As found in previous studies [Lim et al., 1990], photobleached zones along a neurite remained stationary and recovered fluorescence gradually. The lack of movement of the bleached zones suggests that the microtubule cytoskeleton is stationary in elongating DRG neurites, and that microtubules are not transported to the growing tip en masse as polymers.

The gradual return of fluorescence to a bleached zone after photobleaching may be due to the assembly of unbleached x-rhodamine-tubulin subunits onto microtubule ends. It is unlikely that the gradual recovery of fluorescence is due to diffusion of labeled monomers into the bleached area. The rate of diffusion of macro-

molecules in cytoplasm, $D \sim 10^{-8} \text{ cm}^2 \text{ s}^{-1}$ [Salmon et al., 1984], is such that all of the fluorescence recovery that is due to diffusion of x-rhodamine-tubulin subunits into the region would occur within seconds, before the first images were recorded at 1 minute after photobleaching [Okabe and Hirokawa, 1992]. Therefore, we can assume that the gradual recovery of fluorescence to the bleached zone after this first time point is due to gradual replacement of microtubules containing bleached subunits by microtubules containing unbleached tubulin. If there were a substantial amount of labeled monomer nearby that was free to diffuse into the bleached area, it would have moved rapidly into the bleached area by the time the first image was recorded, and the first image would have shown fluorescence in the bleached zone that was above background levels. Since the imaging system was a digital, linearly responding device, the fluorescence intensities that we recorded should be directly proportional to the concentration of x-rhodamine-tubulin.

Quantitative Analysis of Fluorescence Recovery in Neurites and Growth Cones

Our observations of 22 bleached zones made along 15 different neurites that were less than 150 μm in length showed that, except for two cases, bleached areas on shorter neurites always recovered 100% of their fluorescence, regardless of their location along a neurite (see Table I and Fig. 3). These results indicate that virtually all of the microtubules in these neurites were dynamic. Recovery times for bleaches made near growth cones were the shortest. Recovery times of bleached areas along neuritic shafts generally ranged from 50–90 minutes, with a few bleached areas taking as long as 200 minutes to recover fully. However, in the case of longer neurites ($>150 \mu\text{m}$), fluorescence recovery was not always complete. Observations of 19 bleached zones on 13 neurites resulted in 100% recovery of fluorescence of all bleaches in the distal half of the longer neurites, but only 50–80% recovery was observed in 10 of 14 bleaches made in the proximal halves of these neurites, suggesting that there are stable populations of microtubules in proximal regions of longer neurites.

To examine whether there was a relationship between microtubule stability and the distance from the growth cone to a bleached zone, we analyzed in detail the recovery of multiple bleaches (22 total bleaches) made on nine individual neurites or different branch segments of the same neurite process, as shown in the table. The results showed that the distal-most bleached zones always recovered fluorescence faster than more proximal bleached zones on the same neurite, indicating that microtubule turnover is more rapid nearer to the distal end of the neurite.

Figures 4 and 5 show a series of phase contrast and

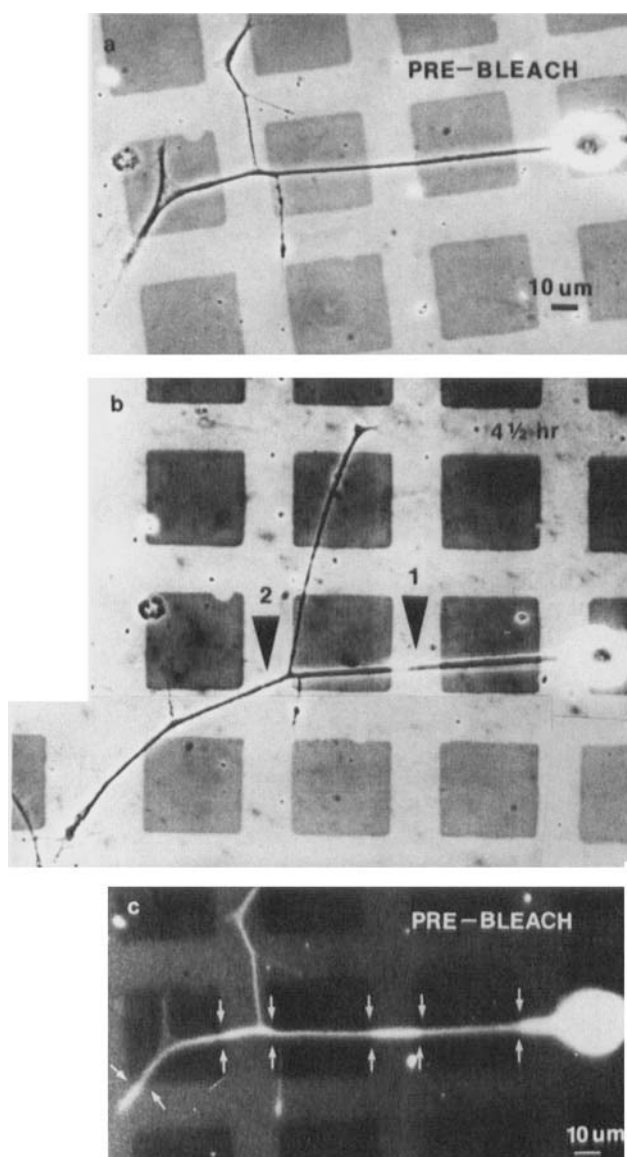


Fig. 4. A neuron that has been photobleached at two points (arrowheads in b) along its neurite continued to grow at normal rates of 10–15 $\mu\text{m}/\text{hour}$ throughout the 4.5-hour experiment shown in Fig. 5, indicating that the neuron remained healthy. (a) Phase contrast image before photobleaching. (b) Phase contrast image 4.5 hours after photobleaching at two branch segments (arrowheads) shows that both distal branches had grown. The length of neurite from the cell body to first branch point did not change. Growth occurred by addition of material to distal branches in all cells measured. (c) Direct rhodamine fluorescence image of the injected neuron. The carbon squares of the grid pattern acted as neutral density filters and reduced the apparent fluorescence, where neurites passed over the carbon-coated areas of the substratum (between arrows). Because of this, all photobleaching was done in the spaces between the carbon squares, and the fluorescence recovery in a bleach zone was measured relative to the fluorescence intensity of the immediate flanking regions of the neurite.

fluorescence images of a branched neurite of a DRG neuron, which elongated a total of 72 μm (from 180–252 μm) during the course of the experiment. Bleaches were placed on the proximal and distal branch segments (arrowheads 1 and 2, respectively). The distal bleached zone recovered within 125 minutes, but full recovery of the proximal bleach took nearly 240 minutes. Figure 6a is a tracing of the fluorescence intensity level along the portions of the neurite that were photobleached. It shows that when the distal bleach reached 100% recovery, the proximal bleach was only 50% recovered. A plot of percent fluorescence recovery over time (Fig. 6b) shows that the rate of recovery was faster for the distal bleach ($t^{1/2} = 55$ minutes) than for the proximal branch ($t^{1/2} = 110$ minutes), suggesting that the microtubules in the distal neurite branch turn over more rapidly.

Bleached zones placed near, or on, growth cones recovered much faster than bleached zones at more proximal sites on the neurites, usually recovering nearly fully within 30 minutes (table and Fig. 3). Figure 7 shows phase and rhodamine-fluorescence images of a bipolar neuron on which a bleached area was made near the base of a growth cone. The bleached zone had almost fully recovered within 18 minutes. Quantitative analysis (Fig. 8) indicates that the $t^{1/2}$ of recovery in this case was 8 minutes.

Incomplete Fluorescence Recovery in More Mature Neurites

Whereas bleached areas that were made anywhere on neurites shorter than about 150 μm always recovered 100% of their fluorescence, recovery of fluorescence was incomplete in most cases of bleached areas that were made on the proximal half of neurite shafts longer than 150 μm . In these cases, the percent recovery of bleaches in the proximal region of the neurite ranged from 50–80% of the initial fluorescence level. This strongly suggests that a subset of stable microtubules, perhaps up to 50% of the total microtubule population in the region, is present in the proximal regions of neurites that have reached a certain length or have elongated for a certain period of time. Despite the incomplete recoveries observed in proximal regions of neurites longer than 150 μm , bleached zones made on the distal halves of these longer neurites always recovered 100% of their initial fluorescence.

Figure 9 shows a DRG neuron whose neurites grew throughout the course of the experiment at an average rate of 20 $\mu\text{m}/\text{hour}$. Phase contrast images taken immediately before (Fig. 9a) and after (not shown) photobleaching two sites show the neurite was initially 319 μm long and elongated to 409 μm by 6 hours after photobleaching. Bleached areas were placed 104 μm and 213

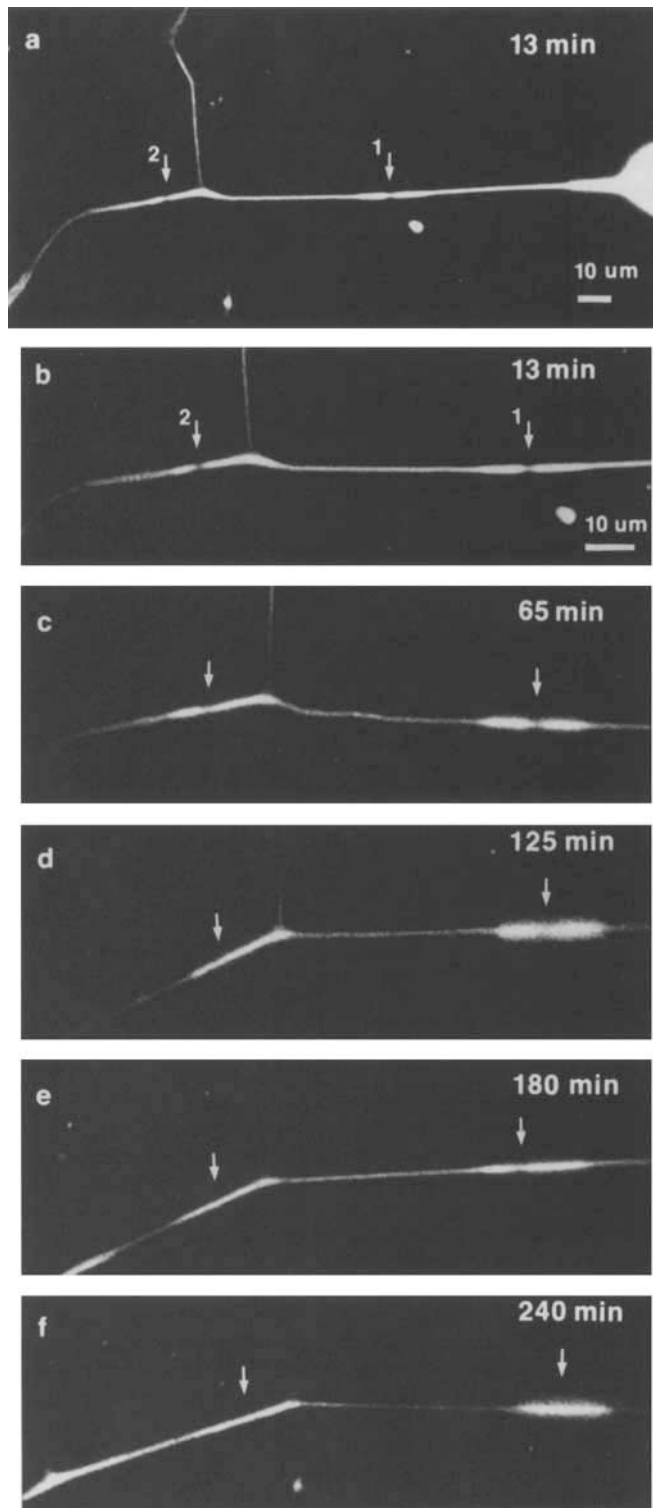


Fig. 5. Recovery of fluorescence along the neurite shown in Fig. 4. The distal bleached zone (arrow 2) recovered its fluorescence more rapidly than an area bleached in the proximal segment, closer to the cell body (arrow 1). (a) The entire neurite at the beginning of the experiment with bleached areas marked with arrows (proximal site-1; distal site-2). The cell body is at the right (see Fig. 4). Subsequent images (b-f) are at slightly higher magnification than in Fig. 4a and show the region with the bleached zones. Bleached zone 2 on the distal branch recovered initial fluorescence by 125 minutes after photobleaching (d), whereas bleached zone 1 remained visible until 240 minutes after photobleaching (f). Both bleached zones were stationary.

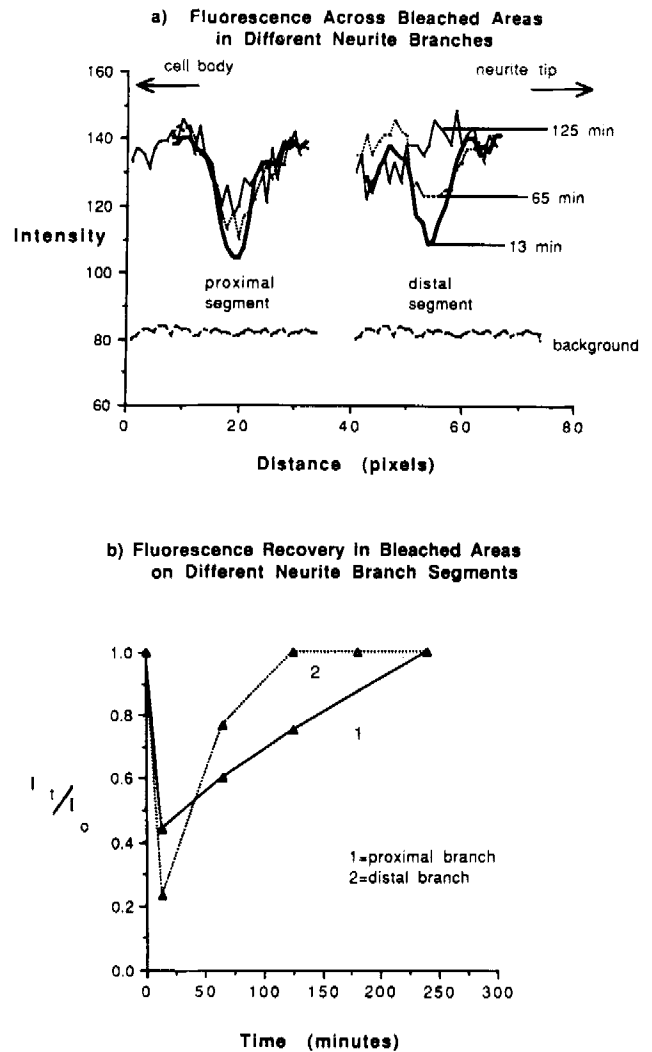
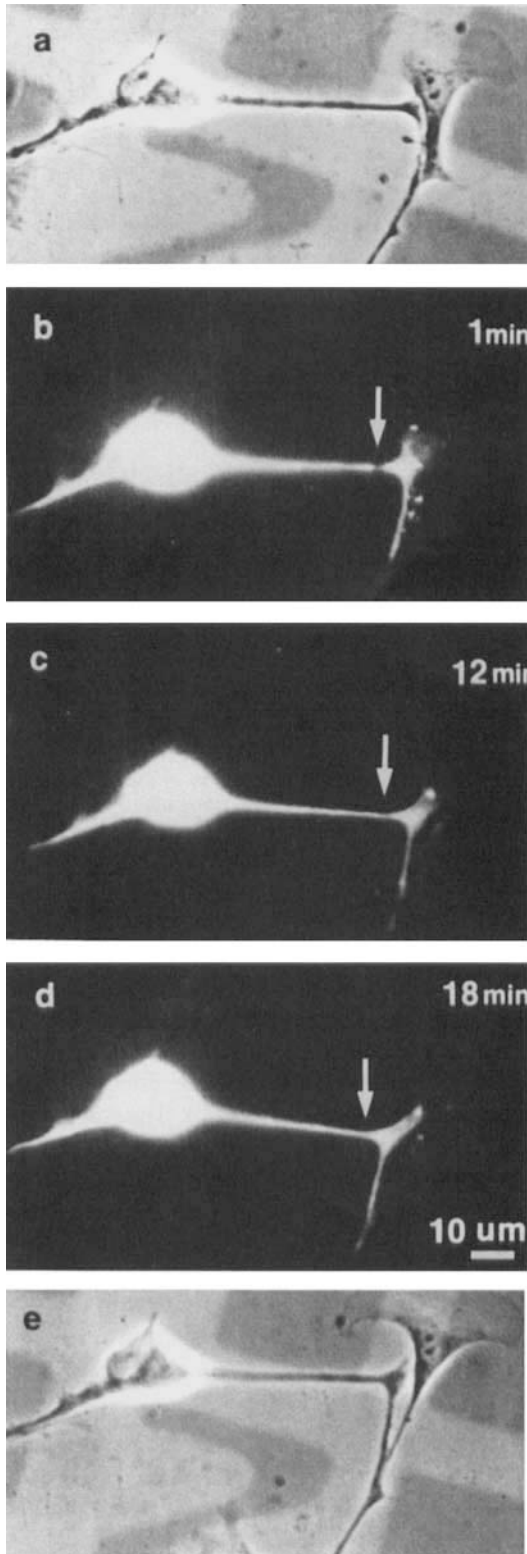


Fig. 6. Quantitative analysis of the fluorescence recovery in the bleached areas of the neurite shown in Fig. 5. The recovery curves indicate that microtubules in the distal neurite turned over faster than microtubules in the proximal segments. (a) Fluorescence intensity was measured at the two regions that were bleached (1, bleach on proximal segment; 2, bleach on distal segment). This measurement included, for comparison, the unbleached neurite areas immediately adjacent to the bleached zones. These measurements were not corrected for background fluorescence. The bottom line ($I = 82$ units) represents the background fluorescence level, which was measured at the level of the substratum in a clear area adjacent to the fluorescent neurite. Each curve represents fluorescence intensity at each pixel point ($3.3 \text{ pixels} = 1 \mu\text{m}$) on a cursor line that was positioned over the neurite in each image, as recorded at 13 minutes (solid bold line), 65 minutes (dotted line), and 125 minutes after photobleaching (solid thin line). Images were taken for 5 hours after photobleaching, but to avoid confusion, only three time points are shown. By 125 minutes the distal bleached area has fully recovered but the proximal site has not fully recovered. By 240 minutes the proximal bleached area has also recovered (trace not shown, but see Fig. 4f). (b) The ratio of fluorescence after photobleaching to fluorescence before bleaching plotted against time after photobleaching (slope = fluorescence recovery rate). (I_t = average fluorescence intensity in the bleached area at time, t ; I_0 = fluorescence intensity in the unbleached neurite area flanking the bleached site). The neurites were bleached to 20–40% of the initial fluorescence level and, in both cases, recovered fully. The distal bleached area (2) recovered at a faster rate ($t^{1/2} = 55$ minutes) than the proximal area (1) ($t^{1/2} = 110$ minutes).

μm from the cell body, making their relative position along the axon equal to 0.33 and 0.67, respectively (0.0 = where the axon emerges from the cell body and 1.0 =



the growth cone). The arrows in Fig. 9b point to each bleached zone.

Rhodamine fluorescent images, along with corresponding phase contrast images to monitor neurite elongation, were stored at time points up to 6 hours after photobleaching. Figure 9b–d shows that by 140 minutes after bleaching, the distal bleached area (arrow 2) had fully recovered, whereas the bleached zone closer to the cell body (arrow 1) had partially recovered, but remained recognizable. In images not included here, this proximal bleached area was still visible even 6 hours after photobleaching. In addition, as seen in cases that showed complete fluorescence recovery, this stable bleached area did not move with respect to the cell body, indicating that these stable microtubules are also stationary and do not move out the neurite.

When analyzing data from the total population of bleached neurites, there was a trend based on the general region of the neurite bleached (see Fig. 3). All bleached areas placed within 20 μm of a growth cone fully recovered their initial fluorescence intensity within 12–45 minutes. Over 90% of bleached areas placed within 105 μm of the growth cone recovered fluorescence fully within 50–100 minutes after photobleaching. Sixty-five percent of bleached sites placed more than 120 μm from the growth cone recovered only 80% or less of their initial fluorescence. The longest time for total recovery was 300 minutes for a bleached zone 59 μm from the soma of a 205 μm neurite (Fig. 3). Variations in recovery time did not appear to be related to neurite elongation rate.

Quantitative analysis of the fluorescence intensity levels (Fig. 10), confirmed these observations. Figure 10a shows a tracing of actual fluorescence intensity measurements made in the regions that were photobleached. Although seven time points were analyzed for up to 6 hours after photobleaching, only three time points are shown here to avoid confusion. At the last time point shown, 140 minutes (solid thin line), the distal bleached zone had fully recovered to the intensity of the unbleached flanking neurite regions. Figure 10b shows the percent fluorescence recovery over time for each bleached area. Comparison of these two recovery curves reveals that both bleached zones reached a maximum

Fig. 7. An area bleached near a growth cone recovered its original level of fluorescence within 18 minutes after photobleaching, much faster than recovery times at proximal sites along a neurite. Phase images before photobleaching (a) and after recovery from fluorescence photobleaching (e) show the neuron was not damaged by the photobleach. Direct rhodamine fluorescence images recorded after photobleaching (b–d) with the time in minutes noted on each image. The bleached area had recovered 85% of its fluorescence by 12 minutes and appeared fully recovered by 18 minutes after photobleaching.

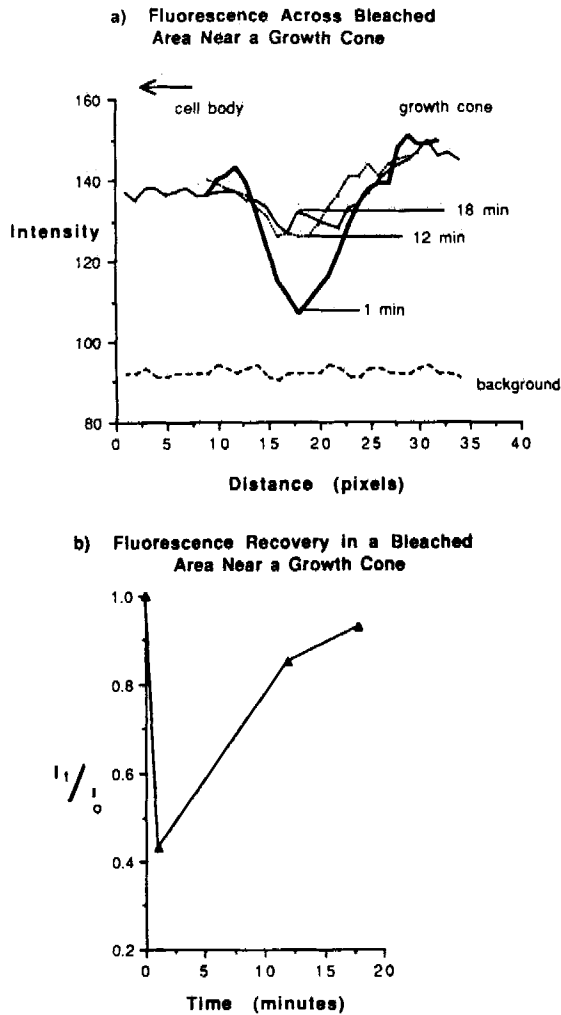


Fig. 8. Quantitative analysis of fluorescence recovery in an area bleached near a growth cone shows that growth cone microtubules turned over rapidly ($t^{1/2} = 8$ minutes). (a) The fluorescence intensity level was measured along the neurite, across the bleached area and into the growth cone at 1, 12, and 18 minutes after photobleaching a $3 \mu\text{m}$ wide area near the base of the growth cone shown in Fig. 7. (b) Analysis of the fluorescence in the bleached area relative to the fluorescence in the flanking region of the neurite. The recovery half-time was eight minutes.

extent of recovery level by 140 minutes after photobleaching, but at this time the distal bleach was 100% recovered and the proximal bleach was only 50% recovered. The recovery curve of the proximal bleach leveled out, and it remained at only 50% recovered up to 6 hours after bleaching. This observation suggests that 50% of the microtubules in this region are significantly more stable than the other microtubules in this area or more distally along the neurite. Further examination of recovery curve 2 also indicates that there may have been more than one component to the recovery in the distal bleached area. Initially, the recovery curve was very steep; fluo-

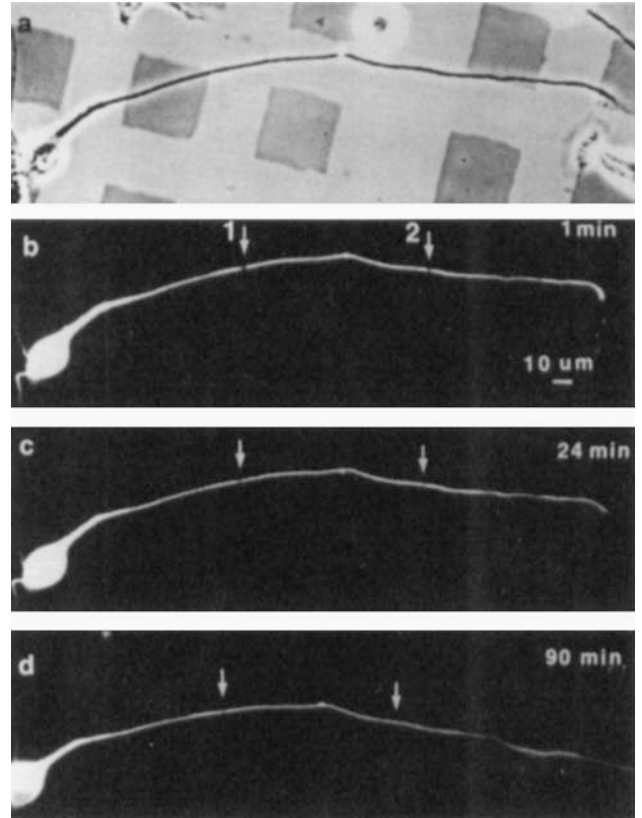


Fig. 9. (a-d) Microtubules in distal regions of the same unbranched neurite turn over more rapidly than those in proximal regions. The unbranched neurite of a DRG neuron, shown here, elongated an average of $20 \mu\text{m}/\text{hour}$. The distal bleached zone (arrow 2) recovered nearly all its initial fluorescence within 90 minutes, whereas the proximal bleach zone (arrow 1) was still visible at 90 minutes. In images recorded later (up to 6 hours after photobleaching), bleach zone 1 was still visible, suggesting that there is an especially stable population of microtubules in the proximal part of this neurite (images not shown).

rescence was 60% recovered by 24 minutes. Then, the rate of recovery leveled off so that the slope of the curve was closer to that of curve 1 for the proximal zone (see also Fig. 6b, distal branch, and 8b). This may mean that there are at least three different classes of microtubules present based on their stability properties: 1) a moderately labile group with $t^{1/2} = 60$ minutes, which is present all along the length of the neurite; 2) a highly labile group with an approximate $t^{1/2} = 13$ minutes at the neurite tip; and 3) a more proximal stable group which does not recover even after 360 minutes.

DISCUSSION

The formation and maturation of neuronal processes depend on the organization of neuritic microtubules. Because microtubules are viewed as dynamic cytoskeletal structures, we considered it important to assess the movements and turnover of microtubules in elongating neurites of embryonic chick DRG neurons, using

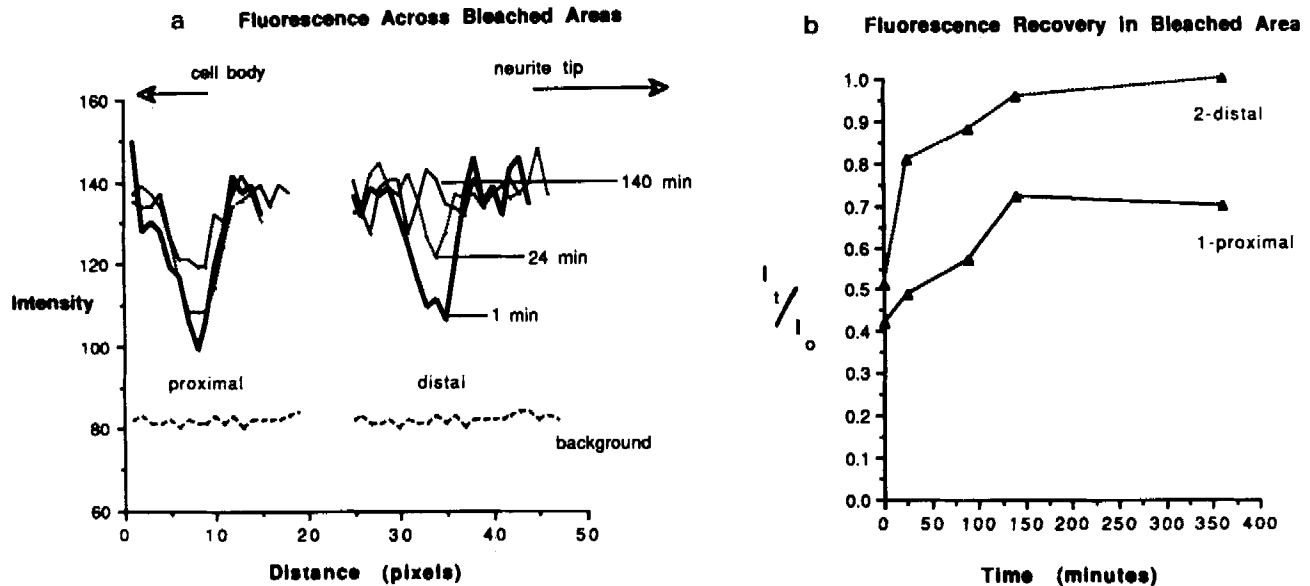


Fig. 10. Quantitative analysis of the fluorescence recovery of the two areas bleached along the unbranched neurite shown in Fig. 9. (a) The fluorescence intensity traces at 1 minute (solid bold line), 24 minutes (dotted line), and 140 minutes (solid thin line) after photobleaching. The distal bleached zone (2) recovered to the intensity level of the unbleached flanking regions within 140 minutes, but the proximal bleached zone (1) did not recover fully. (b) The distal bleached area

(2) was fully recovered by 140 minutes after photobleaching. The proximal bleached area (1) also reached its maximum recovery level by 140 minutes, but it had recovered only 50% of its original fluorescence intensity level, even at 360 minutes after photobleaching when the last observation was made. This suggests that approximately 50% of the microtubules in the proximal region of this neurite were stable and did not turn over.

the techniques of fluorescence recovery after photobleaching. The work reported here extends earlier work from our laboratories [Letourneau, 1982; Lim et al., 1989; 1990]. In addition to providing further confirmation that microtubules are stationary in growing DRG sensory neurites [Lim et al., 1989; 1990; Okabe and Hirokawa, 1990], our evidence suggests there is a distal-to-proximal increase in the stability of the microtubule population along a neurite, changing from predominantly labile microtubules at the growth cone to a high degree of microtubule stability in the proximal regions of neurites.

Our observation of stationary bleached zones at all sites on elongating neurites confirms our previous studies of embryonic chick DRGs [Lim et al., 1990] and is consistent with both photobleaching and photoactivation studies of cultured adult mouse DRGs [Okabe and Hirokawa, 1990, 1992]. Okabe and Hirokawa's recent results [1992] indicate that differences in neuronal types rather than techniques are responsible for the discrepancy between the initial studies of photoactivated tubulin in frog neurons [Reinsch et al., 1991] vs. studies of photobleached tubulin in chick and mouse neurons [Lim et al., 1990; Okabe and Hirokawa, 1990]. Perhaps, microtubules are transported distally in frog neurons and are not transported in significant numbers in mouse and chick neurons because there are different interactions of microtubules with cellular structures that either anchor mi-

croto- tubules to stationary components in chick and mouse neurons or, conversely, permit microtubule transport along with other moving components in frog neurons.

If there were a proximal-to-distal transport of a substantial fraction of labeled microtubules in chick neurites, one should see the fluorescence recovery fill in first on the proximal part of the bleached zone, blurring the edges of the bleached zone. However, we observed that the edges of the bleached zone remained sharp over the time course of recovery, and the fluorescence recovered uniformly across the bleached zone, as far as our methods allowed us to distinguish. This indicates that the recovery process involved events occurring throughout the bleached area, which is also inconsistent with the notion that the distal transport of unbleached microtubules contributes substantially to the recovery of fluorescence.

Recovery of bleached zones means that segments of microtubules consisting of bleached tubulin are replaced by microtubule segments containing unbleached tubulin. If most or all neuritic microtubules are stationary, then what mechanisms could explain the recovery of fluorescence to a stationary bleached zone? Recovery must involve microtubule growth, which might occur by several modes: 1) intercalation of subunits into the microtubule wall [Dye et al., 1992], 2) annealing of short microtubules onto the ends of existing microtubules [Rothwell et al.,

1986], 3) nucleation of new microtubules, and 4) net addition of tubulin to the plus ends of existing microtubules [Cassimeris et al., 1988; Sammak et al., 1987; Sammak and Borisy, 1988a; 1988b; Kirschner and Schulze, 1986; Schulze and Kirschner, 1988]. Although our results do not rule out intercalation or annealing, there is no evidence for these processes occurring in cells. In a series of studies in fibroblasts, monocytes, NGF-treated PC12 cells, and neurons, it was found that microinjected labeled tubulin was added to the plus ends of microtubules and to new microtubules nucleated from the centrosome [Soltys and Borisy, 1985; Sammak and Borisy, 1988b; Kirschner and Schulze, 1986; Okabe and Hirokawa 1988; Cassimeris et al., 1986]. Baas and Ahmad [1992] recently reported that the microtubule assembly in elongating neurites occurs only by the addition of tubulin to the plus ends of stable microtubules. They found no evidence of other microtubule nucleating sites within neurites. In consideration of this evidence, the most likely explanation for the recovery of bleached zones appears to be dynamic instability, the flux of microtubule disassembly and assembly at the plus ends of neuritic microtubules. Another possible mode of recovery is via the nucleation of new microtubules in the perikaryon, followed by terminal addition of tubulin to extend these microtubules into the neurite and through the bleached zones. However, this was probably not a significant activity, because we did not find that recovery of fluorescence was earlier at the proximal side of bleached zones. In addition, bleached zones along the proximal portions of neurites would have recovered more rapidly than distal bleached zones if many new microtubules were growing from the perikaryon. In fact, our results were the opposite, bleached zones at proximal regions of neurites recovered more slowly than distal bleached zones.

Our most significant new finding is the demonstration of a characteristic proximal-distal change in the turnover of microtubules along growing chick embryo DRG neurites. Previous FRAP studies indicated that microtubules at the neurite tip turn over rapidly, while proximally located microtubules in the neurite turn over slower [Lim et al., 1989; Okabe and Hirokawa, 1990]. Our new information indicates that the neuritic microtubules are not a homogeneous population in terms of stability, but rather that the microtubule population varies, so that the proximal regions of neurites longer than 150 μm contain a significant number of microtubules that do not turn over for at least 4 hours. Microtubules in most other cell types do not express such a wide range of stabilities.

It is fitting that the microtubules in locomotory growth cones are dynamic structures. Video microscopic studies of microinjected fluorescent-tubulin provide direct observations of the growth and shrinkage of individual microtubules at the front of active growth cones

[Tanaka and Kirschner, 1991], as previously observed in fibroblast lamellae [Sammak and Borisy, 1988b; Schulze and Kirschner, 1988]. These observations of microtubules in living cells support the concept of dynamic instability [Sammak and Borisy, 1988a; 1988b; Schulze and Kirschner, 1988], although the microtubules did not depolymerize completely to their minus ends, as occurs *in vitro*. Similarly, we found that bleached zones of tubulin at neurite tips ($t^{1/2} = 11 \pm 3$ minutes) recovered at the same rate as was measured in the fibroblast leading edge ($t^{1/2} = 15\text{--}20$ minutes) [Soltys and Borisy, 1985; Sammak and Borisy, 1988b]; $t^{1/2} = 5\text{--}10$ minutes [Schulze and Kirschner, 1988]. These observations of living cells are consistent with immunocytochemical demonstrations that microtubules in growth cones are rich in tyrosinated tubulin [Robson and Burgoyne, 1989; Arregui et al., 1991], which is more prevalent in unmodified newly formed microtubules. In addition, labeling for detyrosinated and acetylated forms of α -tubulin, which is strong in stable microtubules, is diminished in growth cones [Lim et al., 1989; Robson and Burgoyne, 1989; Baas et al., 1991; Dotti and Banker, 1991]. Ultrastructural serial reconstructions indicated that the distal ends of growth cone microtubules are morphologically immature [Cheng and Reese, 1988]. Thus, a variety of evidence supports the view that the microtubule ends that project into growth cones are newly formed and labile.

Quite different from growth cones, microtubules in mature axons are unusually stable, compared to the cytoplasmic microtubules of other cells [reviewed in Bray-Deakin, 1991]. The high stability of neuritic microtubules may be a key characteristic that permits long-term maintenance of far-flung dendritic and axonal processes. Apparently, these mechanisms of axonal microtubule stabilization operate in embryonic neurons, since several sources indicate that elongating neurites contain stable microtubules. These include photobleaching studies [Lim et al., 1990; Okabe and Hirokawa, 1990], such as presented here, labeling of neuritic microtubules for detyrosinated and acetylated tubulin [Robson and Burgoyne, 1989], and resistance of neuritic microtubules to cold and drugs that depolymerize microtubules [Baas and Black, 1990; Baas et al., 1991; Baas and Ahmad, 1992]. Although several means of microtubule stabilization in neurites have been suggested, including posttranslational modifications of tubulin and the actions of several microtubule binding proteins, the molecular mechanisms are not fully understood. Some microtubule stabilization may specifically involve the ends of microtubules to deter the loss of tubulin, while other modifications may act on tubulin subunits generally to stabilize them against depolymerization from an end.

Continuing our previous studies of FRAP in DRG neurites, these studies have found a characteristic proximo-distal change in microtubule turnover. At the neurite tip, microtubule fluorescence recovered with a $t^{1/2}$ of about 10 minutes, further back from the neurite tip recovery time ranged from 60–100 minutes, and in the most proximal region of longer neurites, recovery of fluorescence was usually not complete even after 240 minutes. Our measurements of FRAP at neurite tips and proximal to neurite tips, respectively, are similar to the half times of microtubule stability in cultured sympathetic neurons, as determined by Baas et al. [1991] via analysis of microtubule resistance to nocodazole-induced depolymerization, $t^{1/2} = 3.5$ minutes and $t^{1/2} = 130$ minutes. If we assume that DRG neurites contain two such distinct classes of microtubules, labile and stable, then we can propose that the regional distribution of microtubules among these classes varies so that proximal neurite regions contain stable microtubules, middle regions contain a mix of stable and unstable microtubules, and in distal regions nearly all microtubules turn over rapidly.

Baas and Ahmad [1992] carried their work further to report that the two populations of nocodazole-sensitive and nocodazole-resistant neuritic microtubules are probably not entirely independent, but rather drug-resistant microtubules are stable at their proximal minus ends and are drug-labile at their plus ends. If we propose that a bleached zone recovers its fluorescence through the dynamic instability of microtubule plus ends, then bleached tubulin is lost by depolymerization from the microtubule plus ends, and recovery of fluorescence occurs via assembly of unbleached tubulin that has diffused into the bleached zones. Bleached zones at a neurite tip will include, or be near the unstable plus ends of microtubules that terminate in the growth cone. Consequently, recovery of fluorescence is rapid, as at the front of a fibroblast. Proximal to the neurite tip there are fewer microtubule ends [Letourneau, 1982], and it is more likely that a bleached zone includes partially stabilized regions of microtubules, proximal to the unstable ends. Thus, it will take longer for dynamic instability to replace the bleached tubulin.

This proposal can be developed further to explain the long recovery times that we observed in the proximal regions of neurites $> 150 \mu\text{m}$. In some cases recovery was incomplete after 4 hours. Examination of cytoskeletons of whole-mounted chick DRG neurons revealed that many neuritic microtubules were long, and few microtubule ends were found along the neurites [Letourneau, 1982]. Although some microtubule ends were not visible in the collapsed specimens, a serial thin section analysis of mouse DRG axons also indicated that neuritic microtubules are long, with a mean length of 109

μm [Bray and Bunge, 1981]. Perhaps the proximal regions of longer neurites contain a high proportion of the proximal ends of long microtubules that are stabilized along much of their length. These microtubules may be highly stabilized by stabilizing agents (i.e., enzymes, tau, other MAPs) that enter the neurites from the perikaryon [Bré and Karsenti, 1990]. Dynamic instability may occur at the distal plus ends of these long microtubules, but the bleached tubulin of photobleached sites made at the proximal ends of these long microtubules may be slowly replaced, because the microtubules are almost always rescued from instability before depolymerization ever reaches the proximal bleached zones.

CONCLUSIONS

In summary, these studies confirm that photobleached sites appear to be immobile all along DRG neurites, indicating that neuritic microtubules are stationary in chick neurons. The recovery of bleached zones is rapid at neurite tips, while fluorescence recovery is significantly slower at sites proximal to the growth cone, and at the most proximal regions of longer neurites, a third or more of the initial level of fluorescence does not recover over 4 hours. These results indicate that the relative proportions of dynamic and stable microtubule structures change characteristically along a developing neurite. These changes in microtubule stability may be part of a program of axonal maturation and the eventual cessation of neurite growth when synaptogenesis occurs.

ACKNOWLEDGMENTS

This research was supported by NIH Grants HD19950 to P.C.L. and GM25062 to G.G.B. Dr. Christopher Cypher provided valuable criticism of the manuscript.

REFERENCES

- Arregui, C., Busciglio, J., Caceras, A., and Barra, H.S. (1991): Tyrosinated and detyrosinated microtubules in axonal processes of cerebellar macroneurons grown in culture. *J. Neurosci. Res.* 28:171–181.
- Baas, P.W., and Ahmad, F.J. (1992): The plus ends of stable microtubules are the exclusive nucleating structures for microtubules in the axon. *J. Cell Biol.* 116:1231–1241.
- Baas, P.W., and Black, M.M. (1990): Individual microtubules in the axon consist of domains that differ in both composition and stability. *J. Cell Biol.* 111:495–509.
- Baas, P.W., White, L.A., and Heidemann, S.R. (1987): Microtubule polarity reversal accompanies regrowth of amputated neurites. *Proc. Natl. Acad. Sci. U.S.A.* 84:5272–5276.
- Baas, P.W., Deitch, J.S., Black, M.M., and Banker, G.A. (1988): Polarity orientation of microtubules in hippocampal neurons: Uniformity in the axon and nonuniformity in the dendrite. *Proc. Natl. Acad. Sci. U.S.A.* 85:8335–8339.
- Baas, P.W., Slaughter, T., Brown, A., and Black, M.M. (1991): Microtubule dynamics in axons and dendrites. *J. Neurosci. Res.* 30:134–153.

- Bamburg, J.R., Bray, D., and Chapman, K. (1986): Assembly of microtubules at the tip of growing axons. *Nature (Lond.)* 321: 788-790.
- Bray, D., and Bunge, M.B. (1981): Serial analysis of microtubules of cultured rat sensory neurons. *J. Neurocytol.* 10:589-605.
- Bré, M.H., and Karsenti, E. (1990): Effects of brain-microtubule associated proteins on microtubule dynamics and the nucleating activity of centrosomes. *Cell Motil. Cytoskeleton* 15:88-98.
- Bulinski, J.C., and Gunderson, G.G. (1991): Stabilization and post-translational modification of microtubules during cellular morphogenesis. *BioEssays* 13:285-293.
- Burton, P.R., and Paige, J.L. (1981): Polarity of axoplasmic microtubules in the olfactory nerve of the frog. *Proc. Natl. Acad. Sci. U.S.A.* 78:3269-3273.
- Cambray-Deakin M.A. (1991): Cytoskeleton of the growing axon. In Burgoyne, R.D. (ed.): "The Neuronal Cytoskeleton." New York: Wiley-Liss, Inc., pp. 233-255.
- Cassimeris, L.U., Wadsworth, R.A., and Salmon, E.D. (1986): Dynamics of microtubule depolymerization in monocytes. *J. Cell Biol.* 102:2023-2032.
- Cassimeris, L., Pryer, N.K., and Salmon, E.D. (1988): Real time observations of microtubule dynamic instability in living cells. *J. Cell Biol.* 107:2223-2231.
- Centonze, V.E., and Borisy, G.G. (1989): Applications and limitations of photobleaching and fluorescence imaging. In Herman, B., and Jacobson, K. (eds.): "Optical Microscopy for Biology." New York: John-Wiley and Sons, Inc., pp. 184-194.
- Cheng, T.P.O., and Reese, T.S. (1988): Compartmentalization of anterogradely and retrogradely transported organelles in axons and growth cones from chick optic tectum. *J. Neurosci.* 8:3190-3199.
- Dotti, C., and Banker, G. (1991): Intracellular organization of hippocampal neurons during the development of neuronal polarity. *J. Cell Sci. Suppl.* 15:75-84.
- Dye, R.B., Flicker, P.F., Lien, D.Y., and Williams, R.C. (1992): End-stabilized microtubules observed in vitro: Stability, subunit interchange, and breakage. *Cell Motil. Cytoskeleton* 21: 171-186.
- Gorbsky, G.J., and Borisy, G.G. (1989): Microtubules of the kinetochore fiber turn over in metaphase but not in anaphase. *J. Cell Biol.* 109:653-662.
- Gordon-Weeks, P.R. (1987): The cytoskeletons of isolated, neuronal growth cones. *Neuroscience* 21:977-989.
- Gordon-Weeks, P.R., and Mansfield, S.G. (1991): Assembly of microtubules in growth cones: The role of microtubule-associated proteins. In Letourneau, P.C., Kater, S.B., and Macagno, E.R. (eds.): "The Nerve Growth Cone." New York: Raven Press, pp. 55-64.
- Heidemann, S.R., Landers, J.M., and Hamborg, M.A. (1981): Polarity orientation of axonal microtubules. *J. Cell Biol.* 91:661-665.
- Hoffman, P., and Lasek, R. (1975): The slow component of axonal transport. Identification of major structural polypeptides of the axon and their generality among mammalian neurons. *J. Cell Biol.* 66:351-366.
- Kirschner, M. and Schulze, E. (1986): Morphogenesis and the control of microtubule dynamics in cells. *J. Cell Sci. (Suppl 5):*293-310.
- Lasek, R. (1986): Polymer sliding in axons. *J. Cell Sci. (suppl)* 5:161-179.
- Letourneau, P.C. (1982): Analysis of microtubule number and length in cytoskeletons of cultured chick sensory neurons. *J. Neurosci.* 2:806-814.
- Letourneau, P.C. (1989): Nerve cell shape. In Bronner, F., and Stein, W.D. (eds.): "Cell Shape: Determinants, Regulation, and Regulatory Role." New York: Academic Press, pp. 247-289.
- Lim, S.-S., Sammak, P.J., and Borisy, G.G. (1989): Progressive and spatially differentiated stability of microtubules in developing neuronal cells. *J. Cell Biol.* 109:253-263.
- Lim, S.-S., Edson, K.J., Letourneau, P.C., and Borisy, G.G. (1990): A test of microtubule translocation during neurite elongation. *J. Cell Biol.* 111:123-130.
- Matus, A. (1988): Microtubule-associated proteins: Their potential role in determining neuronal morphology. *Ann. Rev. Neurosci.* 11:29-44.
- Mitchison, T., and Kirschner, M. (1988): Cytoskeletal dynamics and nerve growth. *Neuron* 1:761-772.
- Okabe, S., and Hirokawa, N. (1988): Microtubule dynamics in nerve cells: Analysis using microinjection of biotinylated tubulin into PC12 cells. *J. Cell Biol.* 107:651-664.
- Okabe, S., and Hirokawa, N. (1990): Turnover of fluorescently labelled tubulin and actin in the axon. *Nature (Lond.)* 343:479-482.
- Okabe, S., and Hirokawa, N. (1992): Differential behavior of photoactivated microtubules in growing axons of mouse and frog neurons. *J. Cell Biol.* 117:105-120.
- Petersen, N.O., Felder, S., and Elson, E.L. (1986): Measurement of lateral diffusion by fluorescence photobleaching recovery. In Weir, D.M., (ed.): "Handbook of Experimental Immunology." Oxford: Blackwell, 1:24.1-24.22.
- Reinsch, S.S., Mitchison, T.J., and Kirschner, M. (1991): Microtubule polymer assembly and transport during axonal elongation. *J. Cell Biol.* 115:365-379.
- Robson S.J., and Burgoyne, R.D. (1989): Differential localization of tyrosinated, detyrosinated, and acetylated alpha-tubulins in neurites and growth cones of dorsal root ganglion neurons. *Cell Motil. Cytoskeleton* 12:273-282.
- Rothwell, S.W., Grasser, W.A., and Murphy, D.B. (1986): End-to-end annealing of microtubules in vitro. *J. Cell Biol.* 102:619-627.
- Salmon, E.D., Saxton, W.M., Leslie, R.J., Karow, M.L., and McIntosh, J.R. (1984): Diffusion coefficient of fluorescein-labeled tubulin in the cytoplasm of embryonic cells of a sea urchin: Video image analysis of fluorescence redistribution after photobleaching. *J. Cell Biol.* 99:2157-2164.
- Sammak, P.J., and Borisy, G.G. (1988a): Detection of single fluorescent microtubules and methods for determining their dynamics in living cells. *Cell Motil. Cytoskeleton* 10:237-245.
- Sammak, P.J., and Borisy, G.G. (1988b): Direct observations of microtubule dynamics in living cells. *Nature (Lond.)* 332:742-726.
- Sammak, P.J., Gorbsky, G.J., and Borisy, G.G. (1987): Microtubule dynamics in vivo; a test of mechanisms of turnover. *J. Cell Biol.* 104:395-405.
- Schulze, E., and Kirschner, M. (1988): Microtubule dynamics in interphase cells. *J. Cell Biol.* 102:1020-1031.
- Soltys, B., and Borisy, G.G. (1985): Polymerization of tubulin in vivo: Direct evidence for assembly onto microtubule ends and from centrosomes. *J. Cell Biol.* 100:1682-1689.
- Tanaka, E., and Kirschner, M. (1991): Microtubule behavior in the growth cones of living neurons during axonal elongation. *J. Cell Biol.* 115:345-363.
- Vigers, G.P.A., Coue, M., and McIntosh, J.R. (1988): Fluorescent microtubules break up under illumination. *J. Cell Biol.* 107: 1011-1024.